NIPES

Advances in Engineering Design Technology

Journal homepage: www.nipesjournals.org.ng

Prediction and Optimization of Activated Tungsten Inert Gas Welding Process Parameters using Expert Systems

[1]Osadiaye, N.H., [2]Obahiagbon, K.

[1]Department of Production Engineering, University of Benin, Benin City, Nigeria
[2]Department of Chemical Engineering, University of Benin, Benin City, Nigeria
Email: nosayaba.osadiaye@uniben.edu

ARTICLE INFORMATION

Article history:
Received 26 December 2023
Revised 03 March 2024
Accepted 15 April 2024
Available online 29 May 2024

Keywords*:TIG Welding, Bead penetration, Mild Steel, Response Surface Methodology (RSM), Artificial Neural Network*

https://doi.org/10.5281/10.5281/zenodo.11391850

ABSTRACT

The achievement of bead penetration in Tungsten Inert Gas Welding plays a crucial role in determining the ultimate weld quality. Multiple machining parameters exert an influence on weld bead penetration, hence, making it imperative to find the optimal combination of machining process variables. The present study analysed the optimization of machining variables for the Tungsten Inert Gas Welding method through the utilization of Response Surface Methodology (RSM) and Artificial Neural Network. A design matrix was created for experiment planning, employing the central composite design methodology. Input process parameters encompassed welding current, welding speed, and wire diameter, while the investigation focused on bead penetration as the output variable. Statistical models for response characteristics were established utilizing experimental data. A total of twenty tests were executed according to the design matrix, involving the welding of two mild steel plates sized at 60 x 40 x 10mm. Bead penetration, the primary response variable in this study, was subsequently measured and recorded on the samples. The findings reveals that a combination of 208.22A welding current, 3.02 mm/s welding speed, and a 2.55mm wire diameter yields an optimal bead penetration of 10.3054 mm. In the case of the Artificial Neural Network (ANN), 70% of the data was allocated for training, 15% for validation, and the remaining 15% for the actual test. Based on the results, a regression plot demonstrates an overall R-value of 0.88521. The Response Surface Methodology is chosen as the superior predictive model compared to the Artificial Neural Network because the RSM output aligns more closely with the experimental data than that of the ANN.

1. Introduction

Welding is a fundamental process across a myriad of industries, from manufacturing and construction to aerospace and automotive. The advantages of TIG welding include precision and versatility in joining materials, making it a favored technique in industries where high-quality welds are crucial [1]. Deep penetration in TIG welding is of particular importance, especially when joining thick materials [2]. At the heart of welding's effectiveness lies the concept of bead penetration, a term that encompasses the depth to which the molten filler material melds with the base metal during the welding operation. Bead penetration stands as a critical aspect of welding. It dictates how well the filler material integrates with the base metal and ultimately determines the strength, durability, and quality of the resulting welded joint [3]. Achieving the right depth of bead penetration is a

hallmark of a successful weld. The significance of bead penetration in TIG welding cannot be overstated [4]. Bead penetration, or the depth to which the weld filler material and base metal fuse, directly influences the integrity of welds, the structural strength of the joined materials, and the risk of welding defects [5]. Achieving deep penetration is essential for ensuring strong, reliable welds, particularly when dealing with thicker workpieces [6]. A plethora of factors exert their influence on bead penetration in welding. Among these, welding parameters take center stage. Factors such welding current, voltage, travel speed, and heat input wield significant control over the depth of penetration [7]. Skillful manipulation of these parameters empowers welders to tailor bead penetration to meet specific requirements. Equally crucial is the choice of welding electrode or filler wire. Different electrodes exhibit varying deposition rates and penetration characteristics. Selection is a matter of matching the electrode type and diameter to the welding application at hand [8]. The joint design, including the gap between the base metals, also plays a pivotal role in determining bead penetration. Joint preparation, therefore, must align with the desired penetration depth [9]. Furthermore, the properties of the base metal cannot be overlooked. Material thickness, composition, and thermal conductivity influence how the base metal responds to the welding process and directly impact bead penetration. Measurement of bead penetration entails assessing the depth to which the weld extends into the base metal is typically expressed in millimeters or inches [10]. Figure 1A and 1B represent the Tungsten Inert Gas Welding and diagram view of TIG welding.
Weld inspectors utilize various techniques, including destructive testing and non-destructive methods, to evaluate bead penetration and ensure it meets the specified standards and requirements [11]. The importance of controlling bead penetration cannot be overstated. Inadequate penetration can lead to weld Imperfections like incomplete fusion or fusion's absence, jeopardizing the joint's integrity [12]. Conversely, excessive penetration may cause burn-through and unwanted distortion [13]. Welders must exercise precision and control to achieve the desired level of penetration consistently. Quality assurance in welding hinges on proper bead penetration. Rigorous inspections and testing protocols are implemented to ascertain that welds conform to prescribed standards and maintain structural integrity [14]. Ensuring the right level of penetration is an integral part of delivering high-quality welds across diverse applications. The prediction and optimization of bead penetration in TIG welding represent critical endeavors that aim to achieve deep penetration, ensure weld quality, and minimize the occurrence of defects. The successful attainment of these objectives requires a comprehensive grasp of welding parameters, electrode geometry, and material properties. Advances in predictive models, computational simulations, and experimental techniques continue to contribute to the improvement and refinement of TIG welding processes.

Future research in this domain should concentrate on the development of advanced predictive models that incorporate real-time monitoring and feedback control systems. The present study allows for the adaptive adjustment of welding parameters, optimizing bead penetration dynamically during TIG welding processes. Additionally, the exploration of new electrode materials and innovative shielding gas compositions may open new avenues for optimizing bead penetration, further elevating weld quality and efficiency.

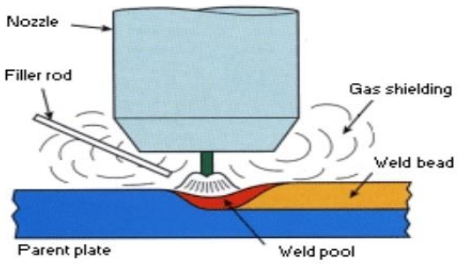

Figure 1: A. Tungsten Inert Gas Welding (fractory.com) B. Schematic view of TIG welding (twi-global.com)

2. Methodology

To effectively address the research problem so as to integrate the different research problem in a logical and coherent way, a plan was chosen and this is the research design. This research experimental analysis of TIG mild steel welds is the main focus of the work, utilizing testing for mechanical attributes, expert systems, analytical and numerical algorithms, and scientific experiment design.

2.1. Design of Experiment

For an accurate polynomial approximation and model development, the design of experiment is needed. There are various experimental design, this consists of the central rotatable designs, and Central composite designed (CCD) and Taguchi. The CCD is selected as the most reliable types of experimental design because of its capacity to handle multi input multi output experimental matrix. The CCD is developed using the following mathematical algorithm.

$$N = 2^n + 2n + k \quad \textbf{(1)}$$

Where, N = Total no. of experiment, n = No. of input parameters, k = No. of centre points = 6.

2.2 Experimental Procedure

The arc welding with tungsten gas technique is among the best welding methods and employed in this study to join the test coupons. The mild steel dish is cleaned and bevelled before the welding process. In this research investigation, shielding gas made entirely of pure Argon was employed to shield the weld specimen from air interaction during the welding process. Mild steel dish employed with a 10mm thickness to create the weld sample specimens. The dish was then cut to size using a power hacksaw. Using sand paper to polish the outer layers and grind the edges, and welding the joins and I recorded the outcome after measurement, the figure below shows the weld samples.

2.3 Response Surface Methodology

Engineers looking for circumstances that will maximize their target process would go for Response Surface Methodology {RSM}. To outline the efficacy of the welding process and choose the most appropriate response, RSM is one of the methods for existing improvement that is widely used. RSM is a combination of analytical and statistical methods that are helpful for developing and foreseeing the interest response that is affected by a variety of input parameters in order to improve the response. A second order polynomial is used to maximize the response surface approach, and the equation is given as follows: response algorithm on full package user-friendly statistical software that makes it simple to compare the results of several approximating functions of different orders.

2.4 Artificial Neural Network

Neural networks are an enormously parallel dispersed processor that has a predisposition to retain experiment data and make it available for use. As a data mining tool, it is employed to find undiscovered patterns in datasets. It matches the brain in two respects. Through a procedure of learning, the network gains knowledge. To retain the knowledge, synapse weights-the degree of intrinsic neuron connection-are applied. The proper w weight is applied to a basic neuron with *R* input. The transfer function's *f* input is composed weighted inputs and distortions added together. To produce their output, neurons are capable of using any transfer function with differentiability. The log-sigmoid transfer function logic is a common component in networks with multiple layers. As the net input of the neuron changes from negative to positive infinitesimal, the logic function generates results between 0 and 1.

3. Results and Discussion

The process parameters and their levels is shown in Table 1, this was used to generate an experimental matrix of twenty runs using the central composite design. Each test constituting the welding current, welding rate and wire diameter utilized to connect two mild steel dishes spanning 60 x 40 x 10mm were carried out. The bead penetration was computed and recorded respectively.

Table 1: Process parameters and their levels

Parameters	**Unit**	**Symbol**	**Coded value**	**Coded value**
			Low(-1)	**High(+1)**
Current	Amp	A	180	220
Speed	Mm/sec	S	2.1	3.5
Diameter	Mm	D	2.1	3.5

3.1 Modelling and Optimization Using RSM

In this research, a second order mathematical model is attempted to be developed using the input parameters welding current (I), welding speed, and wire diameter along with the response parameter bead penetration. Creating the tests necessary for the optimization procedure;

i. The central composite design approach (CCD) was utilized for statistical design of experiments (DOE). Utilizing a statistical tool, the planning and optimization were carried out. Design Expert 7.01 was employed for this case.
ii. A second step involved creating an experimental design matrix with 20 tests and six (6) center points (k), six (6) axial points (2n), and eight (8) factorial points (2^n).

The sum of squares for the sequential model was obtained for the responses' bead penetration in order to confirm the usefulness of the quadratic model for analyzing data from experiments, as demonstrated in Table 2.

Table 2: Sum of squares in a sequential model for bead penetration

	Sum of		Avg	F	p-value	
Origin	Squares	df	Square	Value	Prob. > F	
Mean vs Total	2148.02	1	2148.02			
Linear vs Mean	2.90	3	0.97	4.65	0.0161	
2FI vs Linear	2.06	3	0.69	7.08	0.0046	

Quadratic vs 2FI	1.26	3	0.42	1140.51	< 0.0001	Suggested
Cubic vs Quadratic	3.668E-003	4	9.170E-004	590.94	<0.0001	Aliased
Residual	9.311E-006	6	1.552E-006			
Total	2154.24	20	107.71			

There was no fit test, which was estimated for every answer in order to evaluate whether or not the quadratic model can account for the fundamental variability present in the test results. A framework with a significant lack of fit cannot be used for forecasting. The results of the calculated lack of fit for the bead penetration are shown in Table 3.

Table 3 **Absence of a fit test for bead penetration**

	Sum of		Avg	F	p-value	
Origin	Squares	Df	Square	Value	Prob > F	
Linear	3.32	11	0.30			
2FI	1.26	8	0.16	4.65	0.0161	
Quadratic	3.677E-003	5	7.355E-004	7.08	0.0046	Suggested
Cubic	9.311E-006	1	9.311E-006	1140.51	0.0713	Aliased
Pure Error	0.000	5	0.000	590.94	<0.0001	

From the results of Table 3, in contrast to the cubic polynomial, which showed there was a severe absence of fit, and suggested for model analysis, the quadratic polynomial did not fit the data significantly.
Table 4 displays the model statistics that were calculated for the bead penetration response centered on the model sources.

Table 4: **Statistics for the model's summary bead penetration**

	Std		Adjusted	Predicted		
Origin	Dev	R-Squared	R-Squared	R-Squared	PRESS	
Linear	0.16	0.4656	0.3655	0.0150	6.13	
2FI	0.31	0.7971	0.7034	0.6239	2.34	
Quadratic	0.019	0.9994	0.9989	0.9954	0.029	Suggested
Cubic	1.246E-003	1.0000	1.0000	0.9997	2.052E-003	Aliased

Each entire model's standard deviation, r-squared, adjusted r-squared, predicted r-squared, and predicted error sum of square (PRESS) statistics are displayed in the statistical analysis of model fit. The ideal criteria for identifying the optimal model source are a low standard deviation, R-Squared close to 1, and a PRESS that is comparatively low. According to the findings of Table 4, the cubic polynomial model was aliased, but the quadratic polynomial model was proposed; as a result, it was chosen for this research.
The goodness of fit statistics utilized to evaluate the reliability of the quadratic model are shown in Table 5 based on its ability to decrease bead penetration.

Table 5 **GOF statistics for minimizing bead penetration**

Std. Dev.	0.019	R – Squared	0.9994
Avg	10.36	Adj R - Squared	0.9989
C.V. %	0.19	Pred R - Squared	0.9954
PRESS	0.029	Adeq Precision	163.913

According to Table 4's findings, finding revealed that the "Predicted R-Squared" value of 0.9954 is reasonably consistent with the "Adj R-Squared" value of 0.9989. The measurement of the signal-to-noise ratio is accurate enough. A ratio of at least 4 is preferred. The computed ratio of 163.913,

which was seen in Table 6, denotes a strong signal. This framework could be used to appropriately explore the design area and sufficiently reduce the bead penetration.
The validity of any model is first determined by the findings of a reliable statistical analysis. To evaluate the response surface model's statistical characteristics, the residual probability normal chart for Bead penetration is seen in Figure 2.

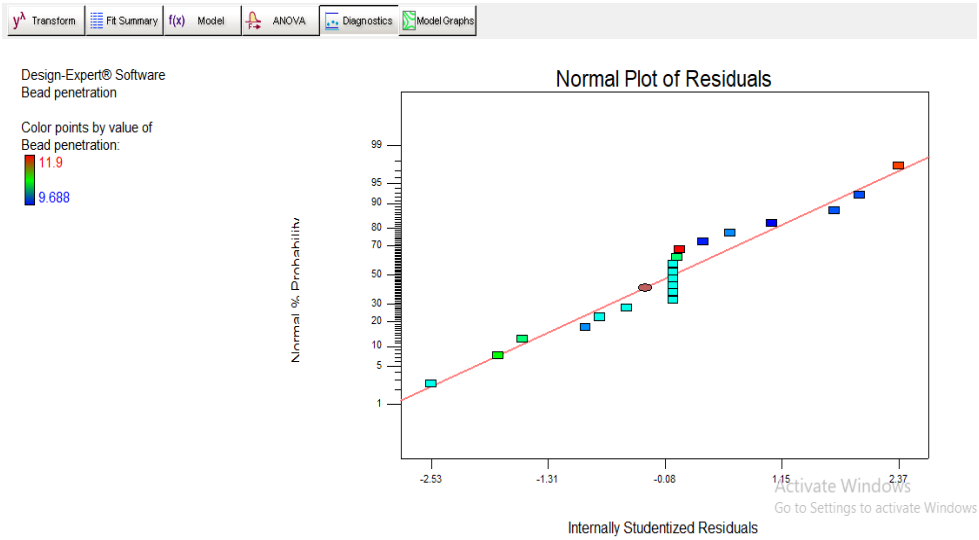

Figure 2: Studentized residuals' normal probability plot for minimizing bead penetration

Despite the modest spread, it might be seen the lines connecting the spots are straight. Aside from the linear trend, there is no clearly defined pattern, such as an "s-shaped" curve. This suggests ensure the residuals are dispersed normally and that data from the output do not need to be transformed for a more thorough investigation.
To detect the presence of mega patterns or expanding variance a plot of residuals and the anticipated was created for the bead penetration which can be seen in Figure 3.

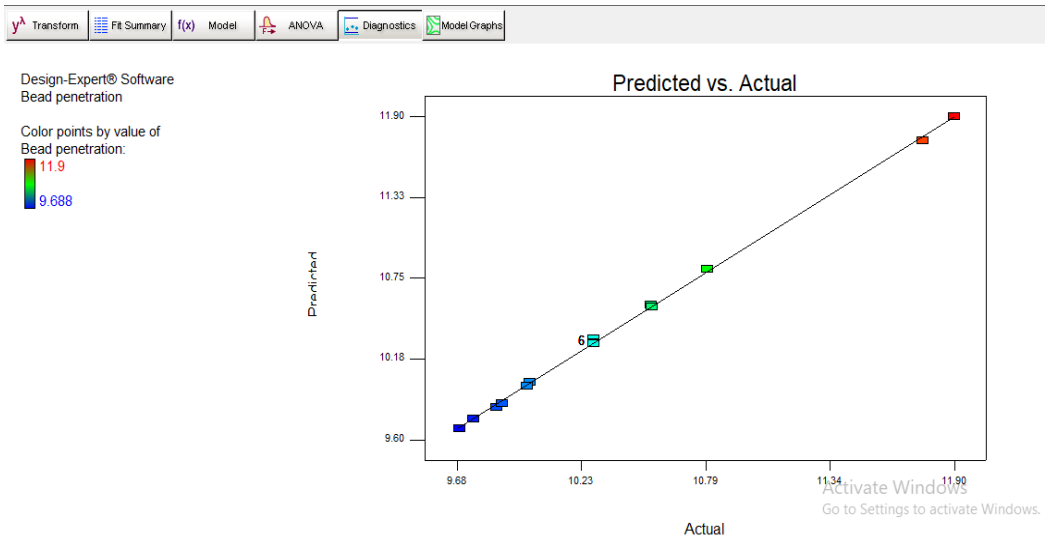

Figure 3: Plot of Residual vs. Predicted for bead penetration

This is the residuals plotted against going up in response values and the variance hypothesis is put to the test. As can be observed, the graph is a random scatter indicating a range of constant the graph's residuals in general.

For each output, a cook's distance chart was made to look for any possible anomalies in the results of the experiment. The extent to which the regression would alter if an outlier were eliminated from the analysis depends on the cook's distance. It is important to investigate a point that sticks out from the others by having a very high distance value. Cook's distance generated for the bead penetration is displayed in Figures 4.

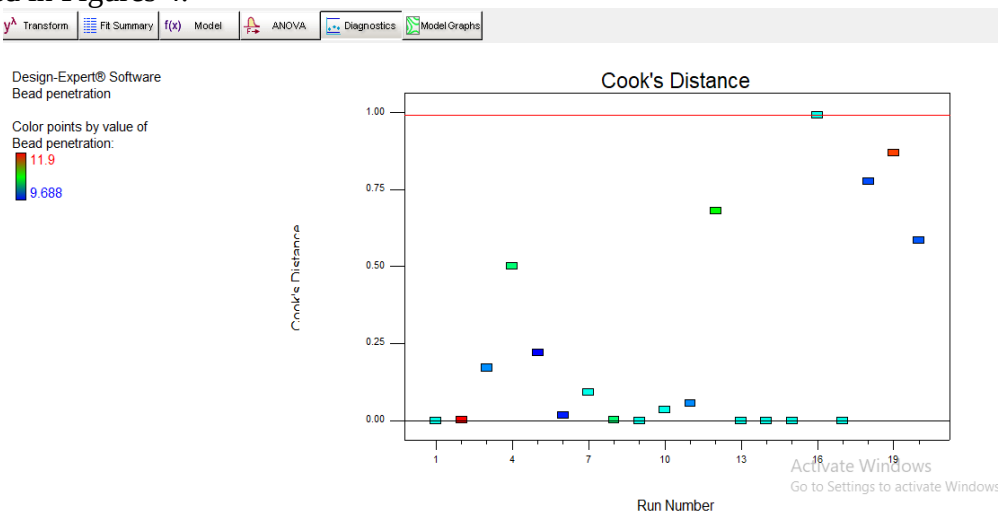

Figure 4 Generated cook's distance for bead penetration

The upper and lower bounds of the cook's distance plot are both 1.00. Outliers are experimental values that are less than or more than the lower or upper bounds and need to be thoroughly studied. Figure 4 findings show the information employed for this study are free of any potential anomalies, demonstrating the sufficiency of the tests.

The 3D surface charts in Figure 5 were created as follows to examine the effects of multiple input parameters on bead penetration.

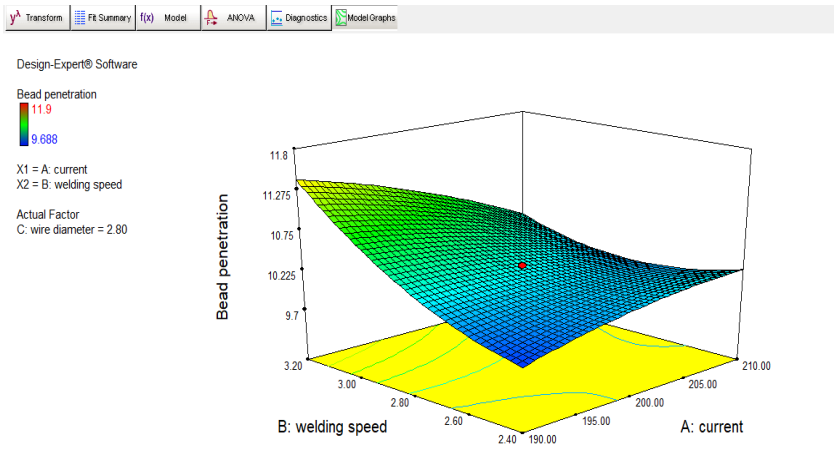

Figure 5: Bead penetration as a function of welding current and speed

The link between welding current and speed on bead penetration is seen in Figure 5. The 3D surface plots in Figure 5 were made using the following technique to examine the effects of wire diameter and welding current on bead penetration. Figure 6A displays the 3D surface plots made in order to explore how welding current and wire diameter affect bead penetration while Figure 6B displays the 3D surface plots to show how the welding speed and wire diameter affects the bead penetration.

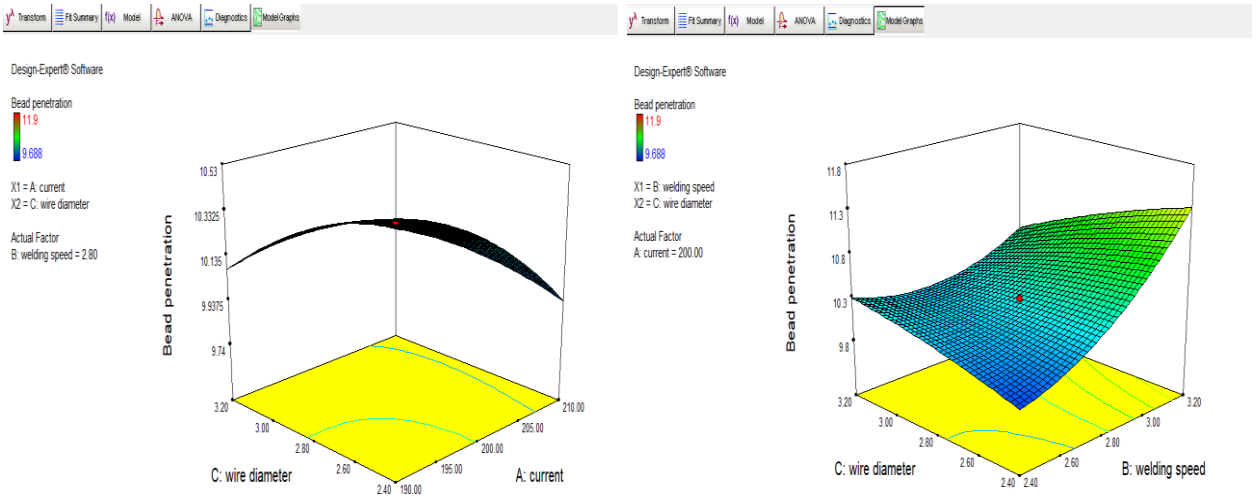

Figure 6 :(A) **Impact of welding current and wire diameter** (B) **Impact of wire diameter and welding speed**

Figure 6 (A) and 6 (B) surface plots illustrates how the relationship between the input factors (welding current, welding speed, and wire diameter) and the outcome factors (bead penetration) is depicted. A three-dimensional surface map was used to provide a greater understanding of the response surface. This image might give a clearer impression of the surface, even though it isn't as helpful as the contour plot for determining outcome values and locations. Darker colors of the curving surface cause a corresponding decrease in bead penetration. The existence of a hued hole at the middle of the upper surface indicated that more dots that were gently tinted for easier recognition went beneath the surface.

Numerical optimization was implemented to determine the desirability of the overall model. In the numerical optimization phase, design expert was used to minimize the droplet bead penetration response as shown in Table 6.

Table 6: The Numerical optimal Solutions

Number	Current	Welding speed	Wire diameter	Bead Penetration	Desirability	
1	**208.22**	**3.02**	**2.55**	**10.3054**	**0.673**	**Selected**
2	210.00	244	2.88	10.2663	0.666	
3	210.00	241	2.87	10.2879	0.665	

3.2 Modelling and prediction using artificial neural network (ANN)

The artificial neural network (ANN) being a predictive model was employed to forecast the response variables outside the realm of investigation. The input matrix contains current weld speed and wire diameter, making it a 3x20 matrix since 20 runs were conducted as shown in the Network training diagram for predicting bead penetration responses in Figure 7.

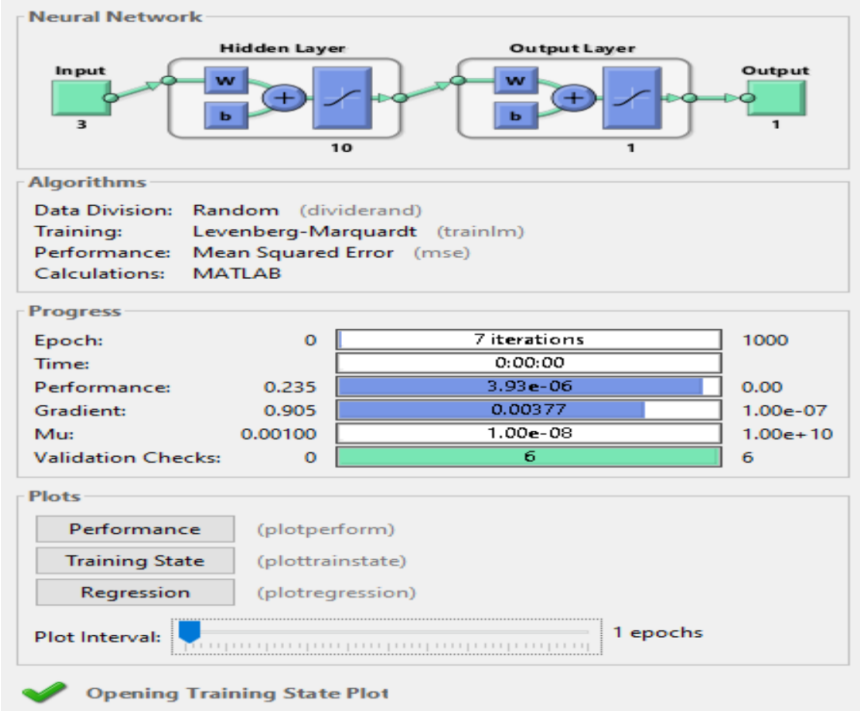

Figure 7: Network training diagram for predicting bead penetration responses

Mean squared error was selected as the performance algorithm, Levenberg-Marquardt as the training method, and data division algorithm was configured to use random (dividerand). In MATLAB software, an epoch can be considered as a finished iteration of your artificial neural network's training process. When all the vectors in your training set are either used or utilized for processing by your training algorithm, this denotes the end of one epoch. Thus, the training method used determines the "real-time duration" of an epoch. Though a total of 7 epochs were employed as iterations are made, as shown in Figure 8, the best forecast for the bead penetration reactions was made at epoch 1. The total amount of epochs used all through the training process is shown in Figure 9.

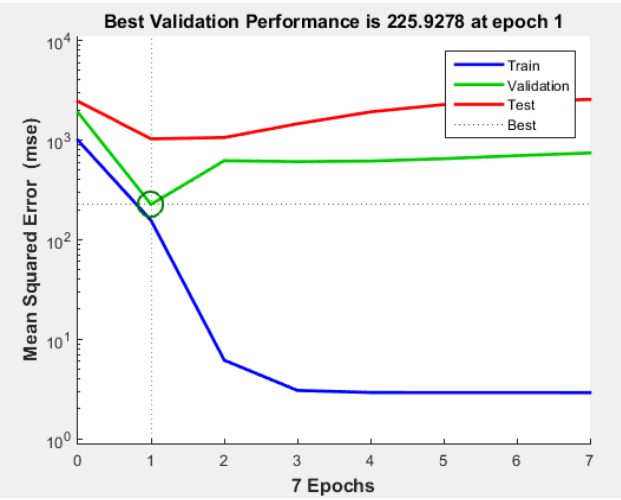

Figure 8: Performance graph of a trained network

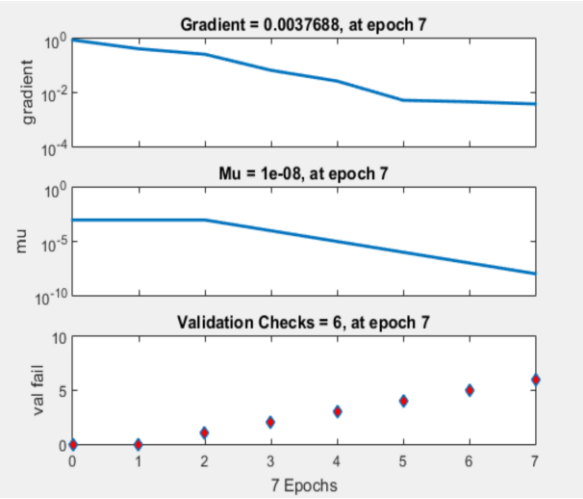

Figure 9: Neural network gradient plot for prediction

One whole algorithm training cycle is represented by one epoch. In Figure 9, out of the 7 epochs used, the most effective estimate was made during the first epoch. The least failure was at epoch 1, as shown by the dotted red lines for validation tests.

Figure 10 displays the training, validation, and testing plot and represents an accurate forecast for the **bead penetration** with a correlation coefficient (R) of over 80%. Each plot's dotted diagonal line denotes the line of best fit, which denotes an accurate forecast and a correlation of 1.

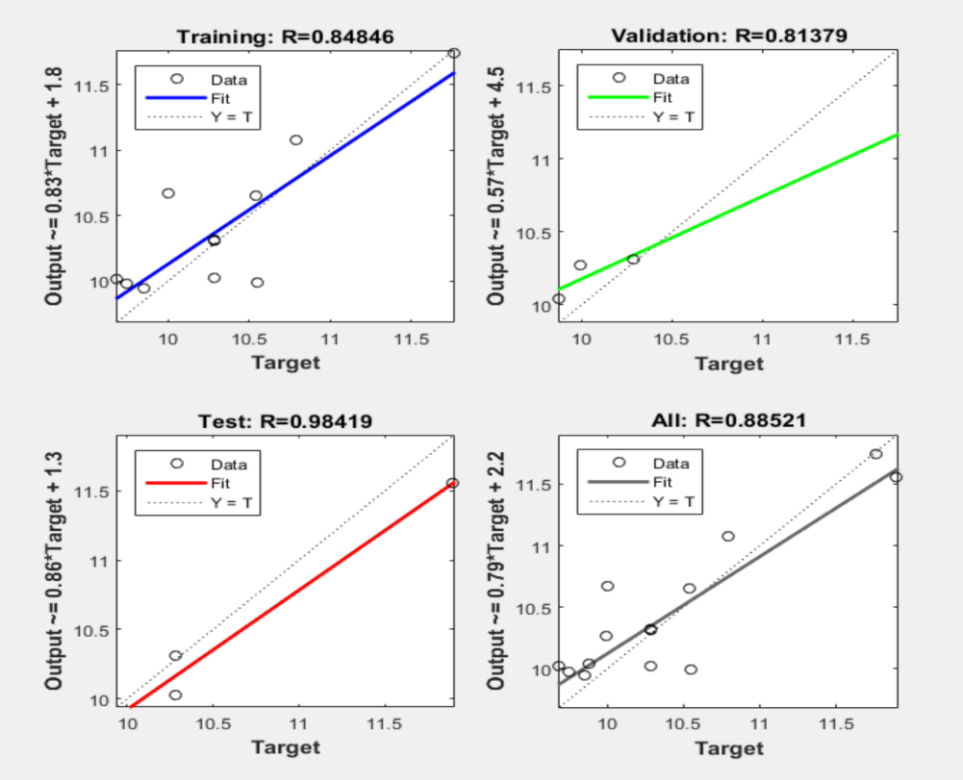

Figure 10: Training, validation, and testing regression plots for bead penetration responses

4. Conclusion

A close examination of the molten metal transfer rate and droplet diameter required for deep penetration during globular to spray was experimented with carefully selecting the welding parameters using these factors; welding current, welding speed and wire diameter to predict and to optimize the MMTR and droplet diameter required for deep penetration with these responses (electrode melting rate, bead penetration, pinch force, droplet diameter, droplet velocity and droplet frequency) using response surface method. Welding current and welding speed are the parameters having the most significant effect on deep penetration and transfer modes; to achieve a better weld with deep penetration and less spatter considering the transfer mode (spray), the current which controls the heat input should be controlled to range of about 208.22Amp. The results from this study show that RSM is an extremely trustworthy and effective instrument for prediction and optimization of the output parameters (bead penetration, electrode melting rate, pinch force, droplet diameter, velocity and frequency) of TIG mild steel weld. RSM's capacity to provide a more accurate explanation for the tests was justified because the predicted R^2 and Adjusted-R^2 had a reasonable agreement which was used as a foundation to defend the equation of the second order polynomial.

Reference

[1] Moi, S. C., Pal, P. K., Bandyopadhyay, A., & Rudrapati, R. (2018). Determination of tungsten inert gas welding input parameters to attain maximum tensile strength of 316L austenitic stainless steel. *Strojnícky časopis-Journal of Mechanical Engineering*, vol.*68* (3), pp.231-248.

[2] Bunaziv, I., Frostevarg, J., Akselsen, O. M., & Kaplan, A. F. (2018). Process stability during fiber laser-arc hybrid welding of thick steel plates. *Optics and Lasers in Engineering*, vol.*102*, pp.34-44.

[3] Gyasi, E. A. (2018). On adaptive intelligent welding: technique feasibility in weld quality assurance for advanced steels.

[4] Silva, R. H. G., dos Santos Paes, L. E., Okuyama, M. P., de Sousa, G. L., Viviani, A. B., Cirino, L. M.,& Schwedersky, M. B. (2018). TIG welding process with dynamic feeding: a characterization approach. *The International Journal of Advanced Manufacturing Technology*, vol.*96*, pp.4467-4475.

[5] Ghosh, A., Bhattachraya, T. K., Deshpande, N. V., & Basak, S. (2019). Microstructural and mechanical properties analysis of plasma ARC welded 316L austenitic stainless steel joints without addition of filler material. *Int. J. Trend Sci. Res. Dev.(IJTSRD)*, vol.*3*, pp.849-865.

[6] Wang, T., Li, Y., Mao, Y., Liu, H., Babkin, A., & Chang, Y. (2022). Research status of deep penetration welding of medium-thick plate aluminum alloy. *The International Journal of Advanced Manufacturing Technology*, vol.*120*(11-12), pp.6993-7010.

[7] DebRoy, T., & Bhadeshia, H. K. D. H. (2021). *Innovations in everyday engineering materials*, pp. 59-60, Springer

[8] Amaral, E. C., Moreno-Uribe, A. M., & Bracarense, A. Q. (2021). Effects of PTFE on operational characteristics and diffusible H and O contents of weld metal in underwater wet welding. *Journal of Manufacturing Processes*, vol.*61*, pp.270-279.

[9] Lu, J., Shi, Y., Bai, L., Zhao, Z., & Han, J. (2020). Collaborative and quantitative prediction for reinforcement and penetration depth of weld bead based on molten pool image and deep residual network. *IEEE Access*, vol.*8*, pp.126138-126148.

[10] Zhang, L., Okudan, G., Basantes-Defaz, A. D. C., Gneiting, R. M., Subramaniam, S., Ozevin, D., & Indacochea, E. (2020). Characterization of GMAW (Gas Metal Arc Welding) Penetration Using Ultrasonics. *Materials*, vol.*13* (10), pp.2307.

[11] Machado, M. A., Rosado, L. F. S. G., Mendes, N. A. M., Miranda, R. M. M., & dos Santos, T. J. G. (2021). New directions for inline inspection of automobile laser welds using non-destructive testing. *The International Journal of Advanced Manufacturing Technology*, pp.1-13.

[12] Aybar, K., & Çakir, F. H. (2023). An experimental study of the friction stir welding of Al 5083 H321 plates by using different process parameters. *Canadian Metallurgical Quarterly*, pp.1-13.

[13] Vasilev, M., MacLeod, C., Javadi, Y., Pierce, G., & Gachagan, A. (2021). Feed forward control of welding process parameters through on-line ultrasonic thickness measurement. *Journal of Manufacturing Processes*, vol.*64*, pp.576-584.

[14] Gan, S., Birrell, L., Robbertze, D., Zhao, B., van Niekerk, E., & Ncubi, L. (2022). Quality control in tailings resource exploration at Havelock Mine, Eswatini. *Journal of the Southern African Institute of Mining and Metallurgy*, vol.*122* (7), pp.347-362.